Available online at www.sciencedirect.com
SCIENCE DIRECT®
International Journal of Heat and Fluid Flow 24 (2003) 816–824
International Journal of HEAT AND FLUID FLOW
www.elsevier.com/locate/ijhff

Investigation of bed shear stresses subject to external turbulence

Nian-Sheng Cheng [a,*], B. Mutlu Sumer [b], Jørgen Fredsøe [b]

[a] School of Civil and Environmental Engineering, Nanyang Technological University, 50, Nanyang Avenue, Blk N1, Singapore 639798, Singapore
[b] Coastal and River Engineering Section (formerly Department of Hydrodynamics and Water Resources, ISVA), MEK, Technical University of Denmark, Building 115, DK-2800 Lyngby, Denmark

Received 5 November 2002; accepted 9 June 2003

Abstract

The fluctuating bed shear stress has largely been investigated only for uniform channel flows and boundary layers. In practical engineering, the flow conditions are often modified due to the presence of various hydraulic structures. To what extent the modification affects the known characteristics of the bed shear stress is not clear. This study presents experimental results of the bed shear stress fluctuations, which are obviously subjected to external turbulence generated by superimposing artificial structures in the open channel flows. The statistical analysis of the measurements shows that the probability density function of the bed shear stress can be described by the lognormal function. Some associated relations concerning higher-order moments, skewness and kurtosis, which are derived from the lognormal function, are further compared with the experimental data. Physical implication of the skewed probability density distribution is finally discussed.

Keywords: Bed shear stress; Fluctuation; Turbulence; Probability density function; Lognormal distribution; Skewness; Kurtosis

1. Introduction

Bedload transport comprises a series of random events associated with motion of bed sediment particles. In describing the motion of the particles in the probabilistic approach, evaluations of probability density functions of the hydrodynamic forces exerted on the particles are essential for conducting relevant analyses. Due to the complexity of the flow around the bed particles, limited information is available on stochastic characteristics of the hydrodynamic forces. This leads to the Gaussian function having often been assumed for many different situations in the previous studies. For example, Einstein and El-Samni (1949) reported that the instantaneous lift force was distributed in the Gaussian fashion. Their result was based on the experiments conducted with a rough bed comprised of hemispheres. The lift force exerted on the hemisphere was simply measured as the pressure difference between the top and bottom of the roughness element. Alternatively, Paintal (1971) applied the Gaussian function to depict the probability density distribution of the dimensionless bed shear stress or Shields number, which is one of the principal parameters included in various formulations related to sediment transport. As the lift force can be expressed in terms of the near-bed velocity, the probability density distribution of the lift force can be derived from that of the near-bed velocity. Cheng and Chiew (1998) performed such a derivation by assuming that the near-bed streamwise velocity was distributed according to the Gaussian function, which leads to an improved pickup probability of sediment entrainment.

The common use of the Gaussian function is also due to its simplicity and good approximation in fitting experimental data related to the near-bed flow conditions for some cases. However, it should be noted that the Gaussian function does not hold for all cases. In commenting the Einstein's bedload function, Yalin (1977) stated that the lift force might distribute differently for different bed conditions and its probability density function may be non-Gaussian in the transitional regime, only tending to be normal in the case of

* Corresponding author. Fax: +65-67910676.
E-mail address: cnscheng@ntu.edu.sg (N.-S. Cheng).

0142-727X/$ - see front matter © 2003 Elsevier Inc. All rights reserved.
doi:10.1016/S0142-727X(03)00088-2

Nomenclature

e	clearance from the lower edge of turbulence generators
I_τ	$(=\tau_{rms}/\tau_{mean})$ relative intensity
K	coefficient of kurtosis
$(\ln\tau)_{mean}$	time-averaged value of the logarithm of the bed shear stress
$(\ln\tau)_{rms}$	rms value of the logarithm of the bed shear stress
Q	flow discharge
S	coefficient of skewness
V	section-averaged velocity
x	distance from turbulence generators to the test section
τ	instantaneous bed shear stress
τ_{mean}	time-averaged mean bed shear stress
τ_n	$(=\tau/\tau_{mean})$ normalised bed shear stress
$(\tau_n)_{mean}$	time-averaged value of the normalised bed shear stress
$(\tau_n)_{rms}$	rms value of the normalised bed shear stress
τ_{rms}	rms value of the bed shear stress

hydrodynamically rough beds. On the other hand, as the lift force is proportional to the square of the near-bed velocity, the probability density functions of the lift force should be non-Gaussian if a near-bed velocity is assumed normally distributed. Obviously, further investigations need to be done to clarify different probability density functions associated with the hydrodynamic forces for various situations. However, it is extremely difficult to perform systematic measurements of the drag and lift forces exerted on the randomly positioned bed particles (e.g., Watters and Rao, 1971; Patnaik et al., 1992; Mollinger and Nieuwstadt, 1996).

Alternatively, the bed shear stress can serve as another important parameter in characterising the flow effect on the motion of the bed particles. It has often been included in many formulations of sediment transport, for example, those related to the critical condition for the initiation of sediment motion and bedload transport rates. Unfortunately, only time-averaged bed shear stress can be measured so far in the presence of the bed particles or rough beds. This is in marked contrast to the fact that much information is available in the literature for the shear stress on a smooth boundary, which enables the measurement of the bed shear stress using the current techniques such as hotfilm, hot-wire, and LDA and its variants. Extensive studies have been done in uniform channel flows and boundary layers by Eckelmann (1974), Blinco and Simons (1974), Girgis (1977), Wietrzak and Lueptow (1994), Colella and Keith (1997), Chew et al. (1998), Miyagi et al. (2000), among others. The measurements conducted in these studies show that the distribution of the bed shear stress is always skewed. Cheng and Law (2003) reported that the probability density distribution derived from the experimental data could be represented well by the lognormal function, rather than the widely used Gaussian function. However, the experimental data collected in the previous studies are usually limited to the simple situations such as uniform open channel flows (e.g., Blinco and Simons, 1974) and boundary layers (e.g., Obi et al., 1996).

It is not clear how the skewed distribution changes and whether the lognormal function is still applicable if the simple flow configurations are altered, for example, in the presence of hydraulic structures in practical engineering. In this study, open channel flows are altered deliberately by introducing external turbulence, which therefore leads to significant modifications to the bed shear stress. With the measured shear stresses, the probability density function and higher-order moments are computed and then compared to theoretical relationships that are derived from the lognormal function. The data used in this study has been obtained in a test program, of which the main purpose was to study the effect of externally generated turbulence on sediment transport. The results of the latter study have been reported in Sumer et al. (2003).

2. Experiments

The experiments were conducted with a tilting flume that was 10 m long and 0.3 m wide at the Technical University of Denmark, MEK, Coastal and River Engineering Section (formerly Department of Hydrodynamics and Water Resources, ISVA). The test section was chosen at 5.6 m from the entrance of the flume. Water was circulated by a pump and the flow rate was controlled with a frequency inverter and monitored using an electromagnetic flow meter. The bed shear stress was measured using a 1-D Dantec hotfilm probe (55R46), which was 0.75 mm long in the transverse direction and 0.2 mm wide in the streamwise direction (Sumer et al., 1993). The probe was mounted flush with the rigid bottom of the flume in the middle of the test section. The calibration was done in situ by first covering the probe with a three-sided calibration channel that was 1 mm deep, 30 mm wide and 180 mm long. Then, the water was pumped through the calibration channel. Because of the small depth, the flow so induced was laminar and thus the bed shear stress could be theoretically computed from the flow discharge. The computed

stress was then related to the hotfilm measurement for the calibration purpose. For each test, the calibration was done twice, one before the test and the other after.

For all the tests, a hydraulically smooth bed was prepared and the water depth at the test section was maintained at 20 cm. The flow rate for each test was so chosen that the time-averaged bed shear stress remained almost constant but the bed shear stress fluctuations varied for different cases. The section-averaged flow velocity varied from 7.0 to 31.2 cm/s, as shown in Table 1. For the undisturbed open channel flow as defined subsequently, the average velocity was 30.7 cm/s and the Reynolds number 26,290.

To have different flow configurations, which affected the bed shear stress fluctuations in the test sections significantly, three turbulence generators were employed to produce external disturbances in the flow. They were a pipe, a short series of grids (referred to as short-grid), and a long series of grids (referred to as long-grid). Both pipe and grid were considered to be typical structures for shedding eddies. Such eddies, when moving downstream, would serve as external turbulence with various scales to affect the bed shear stress measured by the hotfilm probe. Different arrangements were made for the three generators, as shown in Figs. 1–3, respectively. Altogether four series of experiments were conducted in this study.

Series 1: Undisturbed flow. The purpose of this series of experiments was to provide data for the flows without the turbulence generators for comparisons with the other cases. For this case, the velocity profiles were measured using a 1-D laser-Doppler anemometer (LDA) manufactured by Dantec, which was operated in forward scatter mode. The measured velocity profile for the undisturbed flow compares well with the van Driest (1956) function and also the logarithmic law for the large distance from the bed. However, the bed shear stress obtained by fitting the limited velocity data to the

Table 1
Summary of experimental data

Run	Q (l/s)	V (cm/s)	x (or e) (cm)	τ_{mean}/ρ (cm^2/s^2)	τ_{rms}/τ_{mean}	$(\ln \tau_n)_{mean}$	$(\ln \tau_n)_{rms}$
(i) Pipe case							
n2511	11.1	18.49	0	3.002	0.212	−0.022	0.209
n2504	18.7	31.23	10	3.025	1.015	−0.500	1.072
n2614	16.0	26.66	15	2.998	0.802	−0.328	0.879
n2402	15.0	24.94	20	3.054	0.660	−0.199	0.649
n2110	15.3	25.51	30	3.023	0.637	−0.173	0.589
n2602	15.1	25.23	40	3.031	0.591	−0.159	0.575
n2604	16.0	26.66	50	2.969	0.592	−0.154	0.562
n2606	17.4	28.94	60	3.038	0.589	−0.155	0.562
n2608	18.0	30.08	70	3.004	0.541	−0.126	0.501
n2609	18.5	30.77	80	2.963	0.560	−0.131	0.508
(ii) Short-grid case							
n2105	5.7	9.52	0	3.008	0.481	−0.105	0.463
n2103	5.6	9.41	10	3.039	0.491	−0.119	0.505
n2102	5.5	9.24	20	2.994	0.478	−0.107	0.469
o0708	6.1	10.09	30	2.990	0.460	−0.105	0.471
n2009	6.4	10.66	40	2.961	0.487	−0.114	0.488
o0301	6.1	10.09	50	2.988	0.473	−0.109	0.477
o0304	6.6	10.95	60	3.023	0.527	−0.134	0.532
o0701	7.8	12.95	70	3.038	0.528	−0.135	0.534
n2006	9.0	14.95	80	2.969	0.553	−0.152	0.576
n2706	10.1	16.80	90	2.981	0.573	−0.162	0.593
n2708	11.7	19.52	110	2.971	0.571	−0.156	0.577
n2710	13.9	23.23	135	2.975	0.560	−0.154	0.573
n2802	15.1	25.23	168	2.989	0.549	−0.139	0.537
(iii) Long-grid case							
n2002	4.2	7.00	2	2.985	0.354	−0.062	0.359
n1903	5.0	8.33	4	3.069	0.442	−0.100	0.463
o0803	6.2	10.33	6	3.036	0.492	−0.115	0.490
o0804	7.4	12.33	8	3.077	0.519	−0.126	0.513
o1509	8.5	14.17	10	3.000	0.542	−0.139	0.545
o1303	10.0	16.66	12	3.037	0.511	−0.122	0.504
o1305	11.5	19.23	14	3.016	0.484	−0.108	0.466
o1502	12.6	20.94	16	2.997	0.455	−0.098	0.445
o1506	15.1	25.23	18	2.964	0.466	−0.099	0.445
s3001	18.4	30.67	20	3.025	0.442	−0.090	0.424

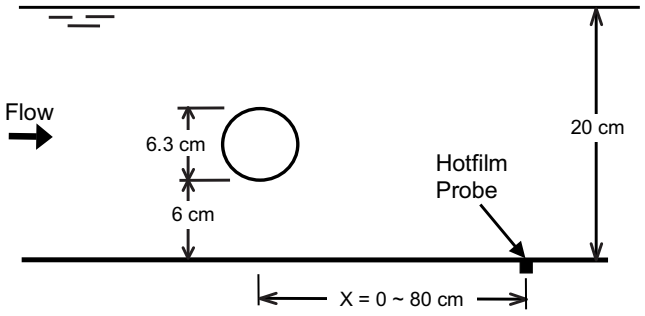

Fig. 1. Definition sketch for pipe case.

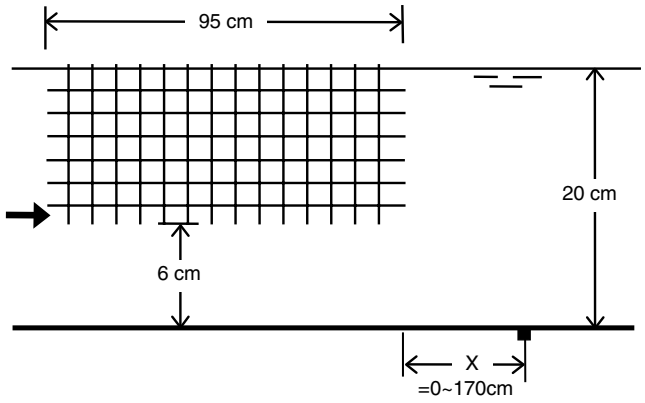

Fig. 2. Definition sketch for short-grid case.

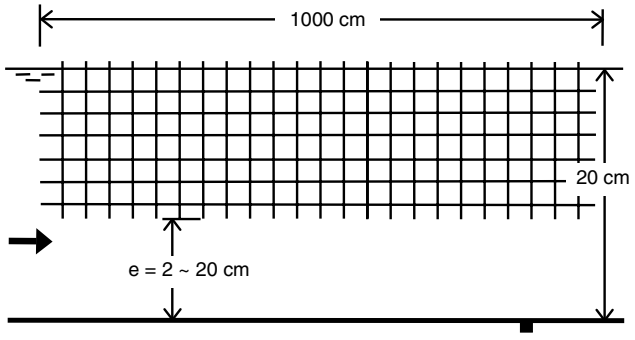

Fig. 3. Definition sketch for long-grid case.

log-law is lower than the hotfilm measurement by approximately 5–10%.

Series 2: Pipe case. For this series, a 30 cm long pipe with a diameter of 6.3 cm was horizontally installed between the side walls of the flume, as shown in Fig. 1. The spacing of the pipe above the bed remained at 6 cm. The longitudinal distance from the section where the pipe located to the test section varied from 0 to 80 cm.

Series 3: Short-grid case. Fig. 2 shows the short-grid, 95 cm long, 29 cm wide and 21 cm high, which was positioned at 6 cm above the bed. The short-grid consisted of 19 pieces of stainless steel perforated plates, which were spaced out 5 cm apart. Each plate was 2 mm thick, having uniformly-distributed square holes (9.5 mm × 9.5 mm). The average porosity for each plate was 69%. The distance from the downstream end of the grid to the test section varied from 0 to 170 cm.

Series 4: Long-grid case. It comprised 10 sections of short-grids, covering the flume in the whole length, as shown in Fig. 3. The clearance between the bed of the flume and the lower edge of the grid ranged from 2 to 20 cm.

It is noted that the four series of experiments conducted in this study were all limited to unidirectional flows, and therefore do not represent other bed shear stress problems.

3. Data analysis

A summary of the experimental results for all the tests is given in Table 1, where the subscripts rms and mean denote the root-mean-square and time-mean values of random variables, respectively; the ratio of τ_{rms} to τ_{mean} is referred to as the relative intensity of the bed shear stress; τ_n is the normalised stress defined as τ/τ_{mean}, and ρ is the density of the fluid.

3.1. Variations of shear stress fluctuations

Figs. 4–6 show variations of the bed shear stress fluctuations for the three cases, respectively. Large variations are found for the pipe case, where the relative intensity of the shear stress, τ_{rms}/τ_{mean}, varies from 0.21 to 1.02. In comparison, the relative intensity is 0.44 for the undisturbed flow, and varies from 0.46 to 0.57 for the long-grid case and from 0.35 to 0.54 for the short-grid case. The difference of the measured fluctuations would reflect the variations in the scale of the generated turbulence. In the near field downstream of the structure, the turbulence scale should be closely related to the

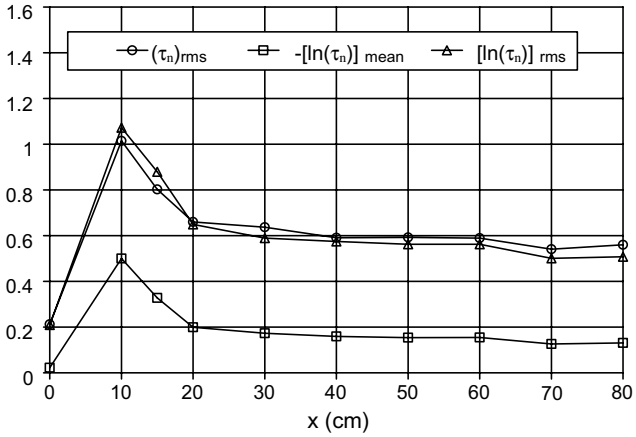

Fig. 4. Variations of relative intensity of bed shear stress, and mean and rms values of $\ln(\tau_n)$ for pipe case.

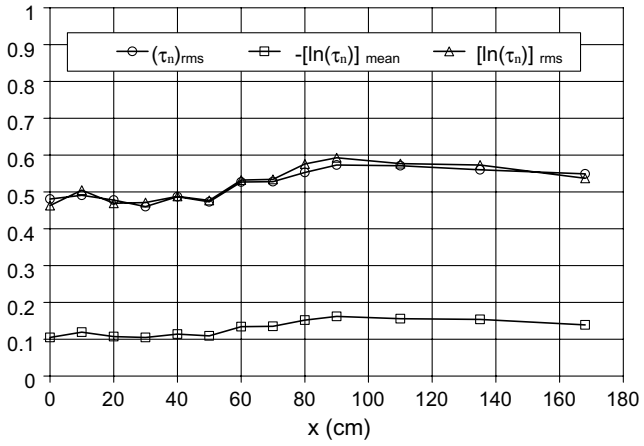

Fig. 5. Variations of relative intensity of bed shear stress, and mean and rms values of $\ln(\tau_n)$ for short-grid case.

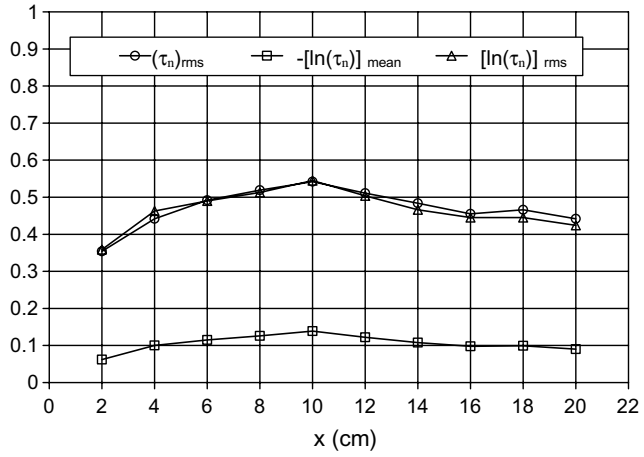

Fig. 6. Variations of relative intensity of bed shear stress, and mean and rms values of $\ln(\tau_n)$ for long-grid case.

dimension of the structure. For the pipe case, the shedding eddies would be larger in size because the pipe diameter is 63 mm, which is much larger than the bar size (2 mm) of the grids. This further implies that the observed stress fluctuation that is more substantial in the presence of the pipe, in particular, when the pipe is not far away from the test section.

In addition, it is noted that the measured relative intensity for the undisturbed flow is slightly higher than the range reported previously, the latter being 0.35–0.40 (e.g., Alfredsson et al., 1988; Naqwi and Reynolds, 1991). No clear explanation for this difference can be made at this stage.

3.2. Probability density distribution

For a unidirectional flow over a hydraulically smooth bed, two basic characteristics of the bed shear stress can be observed from the experiment results. First, the bed shear stress is always positive, implying that no flow reversals occur very near the bed. Second, the distribution of the fluctuating bed shear stress is positively skewed. Cheng and Law (2003) have shown that the skewed distribution can be reproduced with the two-parameter lognormal function, which agrees well with the measured results for the uniform channel flows and boundary layers.

With the lognormal function, the probability density function of the bed shear stress τ can be expressed as

$$f(\tau)=\begin{cases}\dfrac{1}{\sqrt{2\pi}(\ln\tau)_{\mathrm{rms}}\tau}\exp\left\{-\dfrac{1}{2}\left(\dfrac{\ln\tau-(\ln\tau)_{\mathrm{mean}}}{(\ln\tau)_{\mathrm{rms}}}\right)^2\right\} \\ \quad \text{for } \tau>0 \\ 0 \quad \text{for } \tau\leqslant 0\end{cases} \tag{1}$$

where $(\ln\tau)_{\mathrm{mean}}$ = mean value of the random variable $\ln\tau$ and $(\ln\tau)_{\mathrm{rms}}$ = rms value of $\ln\tau$. The two parameters, $(\ln\tau)_{\mathrm{mean}}$ and $(\ln\tau)_{\mathrm{rms}}$, indicate the statistical characteristics of the logarithm of the bed shear stress. Their variations for the three cases of the experiments are shown in Figs. 4–6. It is interesting to note that the two parameters vary in the similar fashion to that for the stress fluctuation. In particular, the magnitude of $(\ln\tau)_{\mathrm{rms}}$ is almost equal to the relative intensity of the shear stress for all the cases, of which more discussions are given subsequently.

Theoretically, $(\ln\tau)_{\mathrm{mean}}$ and $(\ln\tau)_{\mathrm{rms}}$ can be related to τ_{mean} and τ_{rms}, as detailed in Appendix A. Such relationships can also be expressed in terms of the normalised shear stress, $\tau_n=\tau/\tau_{\mathrm{mean}}$, as follows

$$(\ln\tau_n)_{\mathrm{mean}}=-\frac{1}{2}\ln\left[1+(\tau_n)^2_{\mathrm{rms}}\right] \tag{2}$$

$$(\ln\tau_n)_{\mathrm{rms}}=\sqrt{\ln\left[1+(\tau_n)^2_{\mathrm{rms}}\right]} \tag{3}$$

where $(\tau_n)_{\mathrm{rms}}=\tau_{\mathrm{rms}}/\tau_{\mathrm{mean}}$ = relative intensity of the bed shear stress denoted as I_τ. With Eqs. (2) and (3), Eq. (1) can be rewritten as

$$f(\tau_n)=\frac{1}{\sqrt{2\pi\left(1+I_\tau^2\right)}\tau_n}\exp\left[-\frac{\left(\ln\tau_n+\ln\sqrt{1+I_\tau^2}\right)^2}{2\ln\left(1+I_\tau^2\right)}\right] \tag{4}$$

for $\tau_n>0$. Eq. (4) indicates that the probability density function of the normalised stress varies with the fluctuating intensity.

Figs. 7–9 show comparisons of Eq. (4) with the experimental results for the cases of pipe, short-grid, and long-grid, respectively. It can be seen that the measured probability density functions generally agree well with the lognormal function for various fluctuating intensities.

Figs. 10 and 11 show the relationship of the mean and rms values of the normalised shear stress and those of its

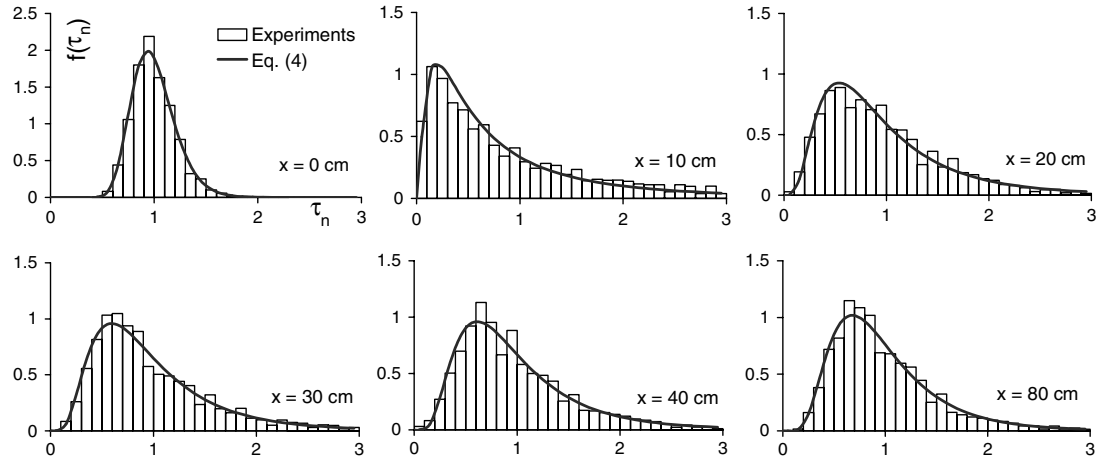

Fig. 7. Probability density function of normalised bed shear stress for pipe case.

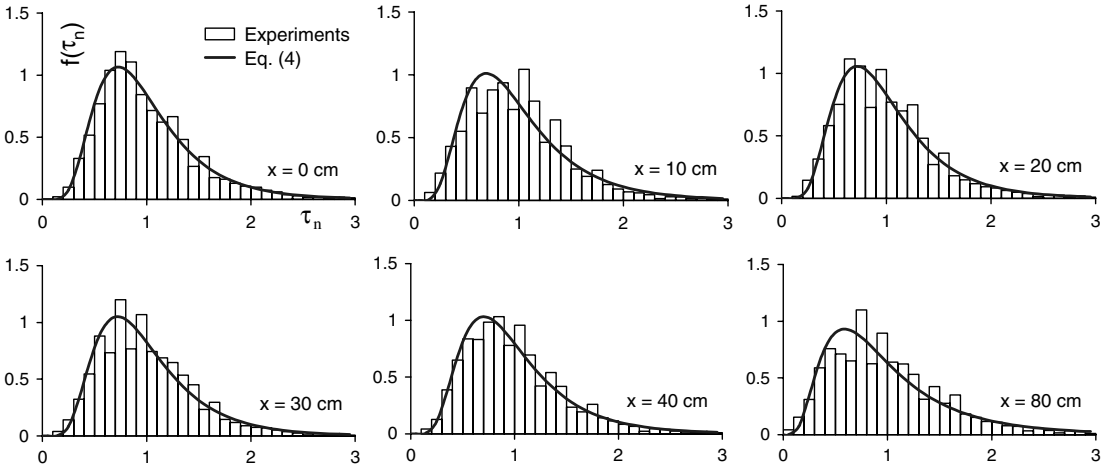

Fig. 8. Probability density function of normalised bed shear stress for short-grid case.

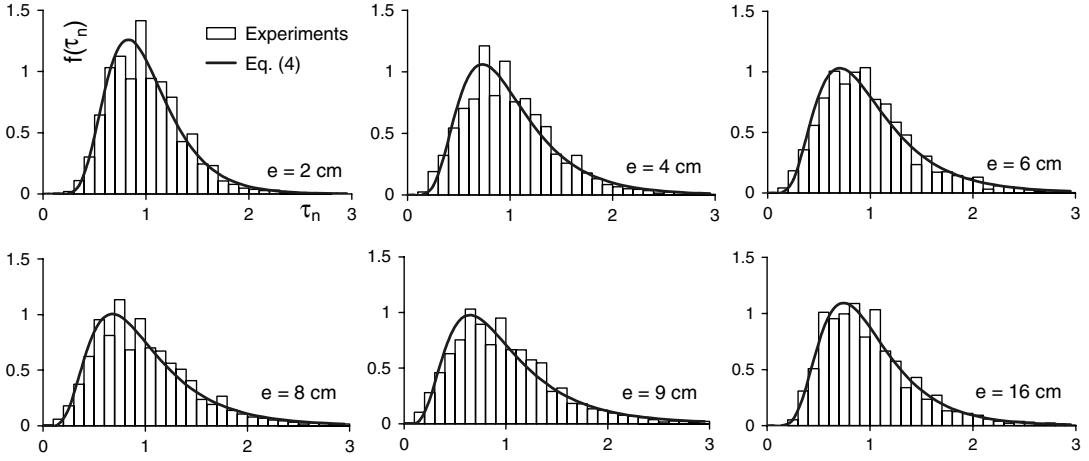

Fig. 9. Probability density function of normalised bed shear stress for long-grid case.

logarithm, $\ln(\tau_n)$, respectively. The theoretical results are computed using Eqs. (2) and (3), respectively. It is interesting to note that the measurements can largely be represented by Eqs. (2) and (3), respectively. However,

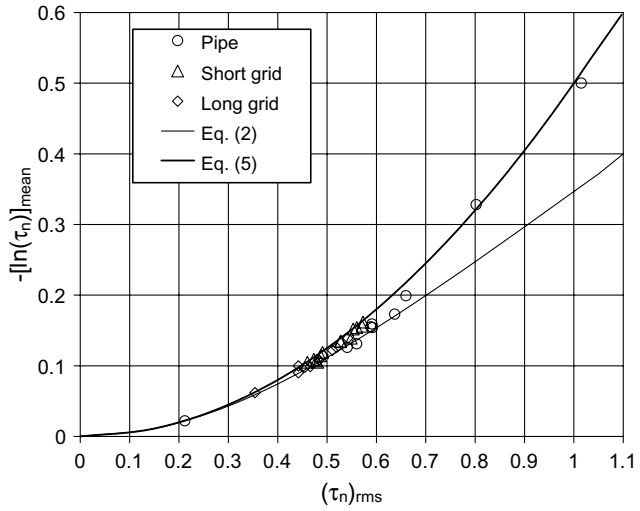

Fig. 10. Relationship of mean value of $\ln(\tau_n)$ and rms value of τ_n.

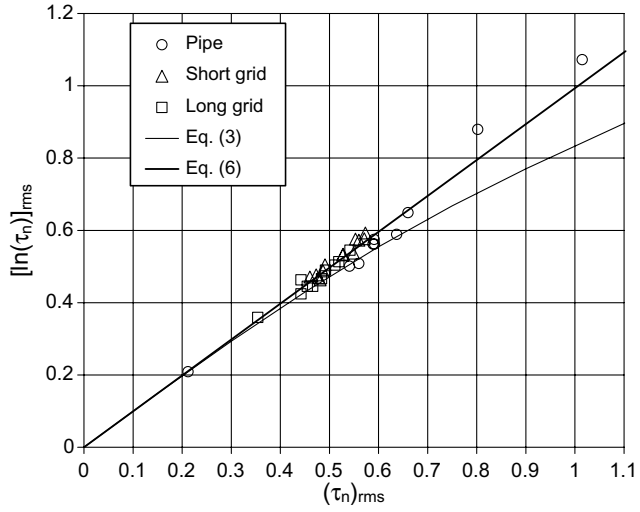

Fig. 11. Relationship of rms values of $\ln(\tau_n)$ and τ_n.

for the pipe case, the experimental data seem to agree better with the following approximate equations:

$$(\ln \tau_n)_{mean} = -\frac{1}{2}(\tau_n)^2_{rms} \tag{5}$$

$$(\ln \tau_n)_{rms} = (\tau_n)_{rms} \tag{6}$$

Eqs. (5) and (6) are derived from Eqs. (2) and (3) for small stress fluctuations by considering the following series expansions:

$$\ln\left[1 + (\tau_n)^2_{rms}\right] = (\tau_n)^2_{rms} - 0.25(\tau_n)^4_{rms} + O[(\tau_n)^6_{rms}] \tag{7}$$

$$\sqrt{\ln\left[1 + (\tau_n)^2_{rms}\right]} = (\tau_n)_{rms} - 0.25(\tau_n)^3_{rms} + O[(\tau_n)^5_{rms}] \tag{8}$$

Obviously, if the terms including $(\tau_n)^3_{rms}$ and higher orders can be ignored, then Eqs. (2) and (3) can be simplified to Eqs. (5) and (6), respectively.

3.3. High-order moments: skewness and kurtosis

The skewness S and kurtosis K are defined, respectively, as

$$S = \frac{\overline{(\tau - \tau_{mean})^3}}{\left[\overline{(\tau - \tau_{mean})^2}\right]^{1.5}} \tag{9}$$

$$K = \frac{\overline{(\tau - \tau_{mean})^4}}{\left[\overline{(\tau - \tau_{mean})^2}\right]^{2}} \tag{10}$$

where the overbars denote the time-average.

With the lognormal function, the above definitions of the skewness and kurtosis can be further expressed in terms of I_τ (Crow and Shimizu, 1988):

$$S = I_\tau^3 + 3I_\tau \tag{11}$$

$$K = I_\tau^8 + 6I_\tau^6 + 15I_\tau^4 + 16I_\tau^2 + 3 \tag{12}$$

From Eqs. (11) and (12), it can be seen that for small I_τ-values, the skewness is approximately equal to zero and the kurtosis 3, implying that the distribution of the fluctuating bed shear stress can be described using the Gaussian function. Comparisons of Eqs. (11) and (12) with the experimental results are given in Figs. 12 and 13, respectively, showing general overestimates with Eqs. (11) and (12) despite the scatter of the measurements. This may be partially due to the fact that the high-order moments of the bed shear stress are usually believed to be significantly subject to the heat loss for the hot-element sensors or insufficient seeding particles

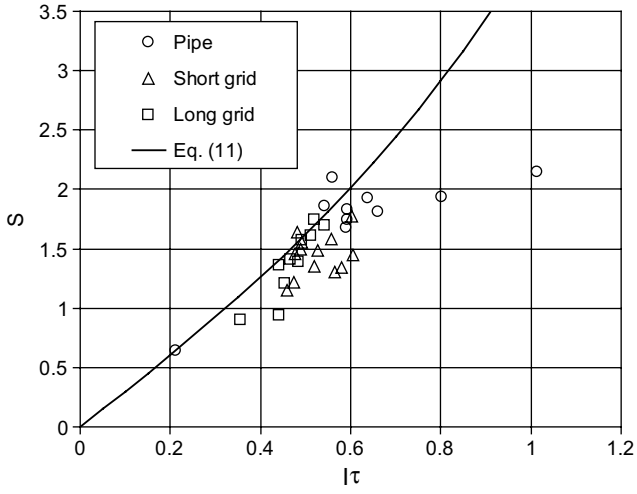

Fig. 12. Relationship of skewness and relative intensity.

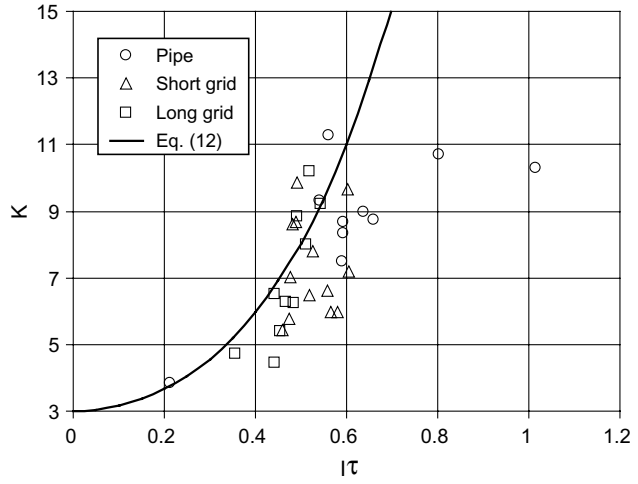

Fig. 13. Relationship of kurtosis and relative intensity.

very close to the bed for the LDA (Wietrzak and Lueptow, 1994; Chew et al., 1998). On the other hand, it is also noted that some significant deviations of the measured skewness and flatness from the predication exist for the pipe case. In particular, the deviations are associated with the pipe which was only 10 and 15 cm upstream of the test section. Therefore, they may result from the direct impact of the eddy shedding from the pipe. Unfortunately, for this particular case, there are only the two data points available from this study. Therefore, further studies are needed so that detailed examination can be made.

In addition, the relationship of S and K is plotted with Eqs. (11) and (12) in Fig. 14 together with the experimental data. Also superimposed in this figure is the following simplified relationship:

$$K = \frac{16}{9}S^2 + 3 \tag{13}$$

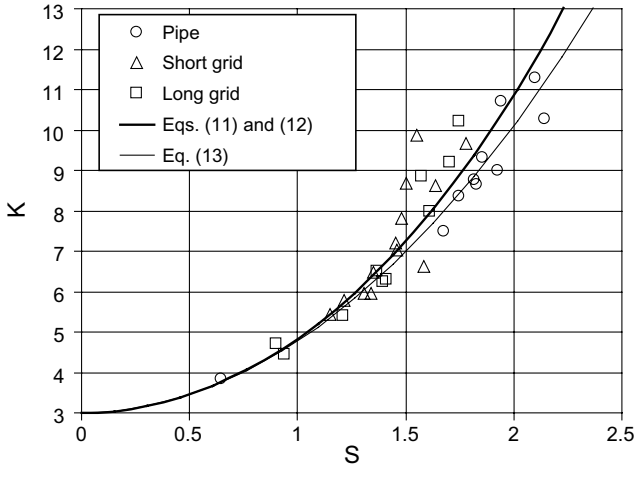

Fig. 14. Relationship of skewness and kurtosis.

which is derived by ignoring the terms included in Eqs. (11) and (12) of which the orders are higher than $O(I_\tau^2)$. Fig. 14 shows that the two theoretical curves are in good agreement with the experimental results.

4. Discussion

From the experimental results obtained in this study, it appears that the probability density distribution of the bed shear stress becomes more skewed when the bed is subjected to external larger-scale turbulence. This phenomenon is evident for the pipe case, in particular, when the pipe is in close proximity of the hotfilm probe or the test section. This is largely because the eddy shed from the pipe in size is of the order of the pipe diameter that is 63 mm. When the pipe is not far from the hotfilm probe, the effect of the eddy shedding is expected more considerable. In contrast, the size of the eddy generated by the grid appears much smaller because the grid bar has a dimension of 2 mm only.

Also demonstrated by the measurements is the fact that the probability density distribution becomes less skewed if the distance from the structure (pipe or grid) to the channel bed at the test section increases. This is because with the increasing distance, the large scale eddy reduces in size when approaching the bed at the test section.

On the other hand, it should be noted that the measured probability density distribution may also be subjected to the performance of the hotfilm probe. As mentioned earlier by Alfredsson et al. (1988), the heat transfer from the probe to substrate may be insensitive to rapid shear stress fluctuations because of the large thermal inertia of the substrate. Therefore, the measured probability density distribution may deviate from the real distribution due to the difference between static and dynamic responses of the hotfilm probe.

5. Conclusions

In this study, various external structures are superimposed in open channel flows to generate additional turbulence. This causes that the bed shear stress fluctuates markedly in comparison with those for the condition of uniform channel flows or boundary layers. The shear stresses were measured with a 1-D hotfilm probe. The statistical analysis of the measurements shows that the probability density distribution of the fluctuating stress can be described effectively using the lognormal function. The skewness and kurtosis generally depend on the relative intensity of the shear stress, and thus are interrelated. The interrelationship that is derived from the lognormal function agrees well with the experimental data.

Acknowledgements

N.-S. Cheng acknowledges the assistance of the technical personnel at the laboratory of Coastal and River Engineering Section, MEK, Technical University of Denmark. This study has been partially supported by the research program "Coast and Tidal Inlets" of the Danish Technical Research Council (STVF).

Appendix A. Derivation of Eq. (4)

In terms of the probability density function $f(\tau)$, τ_{mean} can be computed as

$$\tau_{\text{mean}} = \int_{-\infty}^{\infty} \tau f(\tau)\,\mathrm{d}\tau \tag{A.1}$$

and τ_{rms} can be defined according to

$$\tau_{\text{rms}}^2 = \int_{-\infty}^{\infty} \tau^2 f(\tau)\,\mathrm{d}\tau - \tau_{\text{mean}}^2 \tag{A.2}$$

Substituting Eq. (1) into Eqs. (A.1) and (A.2), respectively, yields

$$\tau_{\text{mean}} = \exp\left[(\ln\tau)_{\text{mean}} + \frac{1}{2}(\ln\tau)_{\text{rms}}^2\right] \tag{A.3}$$

and

$$\tau_{\text{rms}} = \tau_{\text{mean}}\sqrt{\exp\left[(\ln\tau)_{\text{rms}}^2\right] - 1} \tag{A.4}$$

From Eq. (A.4), one gets

$$(\ln\tau)_{\text{rms}} = \sqrt{\ln\left(1 + I_\tau^2\right)} \tag{A.5}$$

Then, substituting Eq. (A.5) into Eq. (A.3) yields

$$(\ln\tau)_{\text{mean}} = \ln\left(\frac{\tau_{\text{mean}}}{\sqrt{1 + I_\tau^2}}\right) \tag{A.6}$$

With Eqs. (A.5) and (A.6), Eq. (1) can be rewritten as

$$f(\tau) = \frac{1}{\sqrt{2\pi\left(1 + I_\tau^2\right)}\tau}\exp\left[-\frac{\left(\ln\frac{\tau}{\tau_{\text{mean}}} + \ln\sqrt{1 + I_\tau^2}\right)^2}{2\ln\left(1 + I_\tau^2\right)}\right] \tag{A.7}$$

for $\tau > 0$. In terms of the normalised stress, Eqs. (A.5)–(A.7) can be changed to Eqs. (2)–(4), respectively.

References

Alfredsson, P.H., Johansson, A.V., Haritonidis, J.H., Eckelmann, H., 1988. The fluctuating wall shear stress and the velocity field in the viscous sublayer. Phys. Fluids 31 (5), 1026–1033.

Blinco, P.H., Simons, D.B., 1974. Characteristics of turbulent boundary shear stress. J. Eng. Mech. Div. ASCE 100 (2), 203–220.

Cheng, N.S., Chiew, Y.M., 1998. Pickup probability for sediment entrainment. J. Hydr. Eng. ASCE 124 (2), 232–235.

Cheng, N.S., Law, A.W.K., 2003. Fluctuations of turbulent bed shear stress. J. Eng. Mech. ASCE 129 (1), 126–130.

Chew, Y.T., Khoo, B.C., Lim, P.C., Teo, C.J., 1998. Dynamic response of a hot-wire anemometer. Part II: A flush-mounted hot-wire and hot-film probes for wall shear stress measurements. Meas. Sci. Technol. 9, 764–778.

Colella, K.J., Keith, W.L., 1997. Measurements of wall shear stress fluctuations beneath a turbulent boundary layer. In: Turbulent Flows, The 1997 ASME Fluids Engineering Division Summer Meeting, vol. 1. American Society of Mechanical Engineers, Fluids Engineering Division (Publication) FED, New York, USA, pp. 1–5.

Crow, E.L., Shimizu, K., 1988. Lognormal Distributions: Theory and Applications. Marcel Dekker, Inc., New York.

Einstein, H.A., El-Samni, E.A., 1949. Hydrodynamic forces on a rough wall. Rev. Mod. Phys. 21 (3), 520–524.

Eckelmann, H., 1974. The structure of the viscous sublayer and the adjacent wall region in a turbulent channel flow. J. Fluid Mech. 65 (3), 439–459.

Girgis, R.N.M.A., 1977. Transport of fine bed sand by laminar and turbulent water flow. Ph.D. thesis, Department of Civil and Municipal Engineering, University College, University of London.

Miyagi, N., Kimura, M., Shoji, H., Saima, A., Ho, C.M., Tung, S., Tai, Y.C., 2000. Statistical analysis on wall shear stress of turbulent boundary layer in a channel flow using micro-shear stress imager. Int. J. Heat Fluid Flow 21, 576–581.

Mollinger, A.M., Nieuwstadt, F.T.M., 1996. Measurement of the lift force on a particle fixed to the wall in the viscous sublayer of a fully developed turbulent boundary layer. J. Fluid Mech. 316, 285–306.

Naqwi, A.A., Reynolds, W.C., 1991. Measurement of turbulent wall velocity gradients using cylindrical waves of laser light. Exp. Fluids 10, 257–266.

Obi, S., Inoue, K., Furukawa, T., Masuda, S., 1996. Experimental study on the statistics of wall shear stress in turbulent channel flows. Int. J. Heat Fluid Flow 17 (3), 187–192.

Paintal, A.S., 1971. A stochastic model of bed load transport. J. Hydr. Res. 4, 527–554.

Patnaik, P.C., Vittal, N., Pande, P.K., 1992. Drag coefficient of a stationary sphere in gradient flow. J. Hydr. Res. 30 (3), 389–402.

Sumer, B.M., Arnskov, M.M., Christiansen, N., Jørgensen, F.E., 1993. Two-component hot-film probe for measurements of wall shear stress. Exp. Fluids 15, 380–384.

Sumer, B.M., Chua, L.H.C., Cheng, N.S., Fredsøe, J., 2003. Influence of turbulence on bed load sediment transport. J. Hydr. Eng. ASCE 129 (8), 585–596.

Watters, G.Z., Rao, M.V.P., 1971. Hydrodynamic effects of seepage on bed particles. J. Hydr. Div. ASCE 97 (3), 421–439.

Wietrzak, A., Lueptow, R.M., 1994. Wall shear stress and velocity in a turbulent axisymmetric boundary layer. J. Fluid Mech. 259, 191–218.

Yalin, M.S., 1977. Mechanics of Sediment Transport, second ed. Pergamon Press, Oxford, England.